Block of an ether-a-go-go-Like K$^+$ Channel by Imipramine Rescues *egl-2* Excitation Defects in *Caenorhabditis elegans*

David Weinshenker,[1,2] **Aguan Wei,**[3] **Lawrence Salkoff,**[3,4] **and James H. Thomas**[1]

[1]*Department of Genetics, and* [2]*Howard Hughes Medical Institute and Department of Biochemistry, University of Washington, Seattle, Washington 98195, and* [3]*Departments of Anatomy and Neurobiology and* [4]*Genetics, Washington University School of Medicine, St. Louis, Missouri 63110*

K$^+$ channels are key regulators of cellular excitability. Mutations that activate K$^+$ channels can lower cellular excitability, whereas those that inhibit K$^+$ channels may increase excitability. We show that the *Caenorhabditis elegans egl-2* gene encodes an eag K$^+$ channel and that a gain-of-function mutation in *egl-2* blocks excitation in neurons and muscles by causing the channel to open at inappropriately negative voltages. Tricyclic antidepressants reverse *egl-2(gf)* mutant phenotypes, suggesting that EGL-2 is a tricyclic target. We verified this by showing that EGL-2 currents are inhibited by imipramine. Similar inhibition is observed with the mouse homolog MEAG, suggesting that inhibition of EAG-like channels may mediate some clinical side effects of this class of antidepressants.

Key words: eag; K$^+$ channel; tricyclic; antidepressant; imipramine; Caenorhabditis elegans; egl-2

K$^+$ channels are key regulators of membrane excitability and are responsible for a number of identified channelopathies underlying neurological and cardiac disorders (Adelman et al., 1995; Curran et al., 1995; Vetter et al., 1996; Wang et al., 1996). In addition, some clinically used drugs may act via K$^+$ channel blockade (Sanguinetti and Jurkiewicz, 1990). *Caenorhabditis elegans* contains a full complement of K$^+$ channel gene families (Wei et al., 1996), and a number of K$^+$ channel mutants have been identified (Elkes et al., 1997; Johnstone et al., 1997; our unpublished data). Behavioral and pharmacological studies of these mutants may provide insight into the genetic and mechanistic basis of K$^+$ channel dysfunction *in vivo*.

Here we report that the behavioral defects in the *C. elegans egl-2* mutant are caused by a gain-of-function (*gf*) mutation in an eag-like K$^+$ channel. eag K$^+$ channels are encoded by one of three distinct subfamilies of genes (eag, erg, and elk), which comprise the *ether-a-go-go* (EAG) extended gene family (Warmke and Ganetzky, 1994; Ganetzky et al., 1999). Members of the EAG family of K$^+$ channels generally produce noninactivating, voltage-dependent potassium currents, characterized by accentuated modulation by internal (Bruggemann et al., 1993; Stansfeld et al., 1996) and external (Terlau et al., 1996; Schonherr et al., 1999) divalent cations. Amino acid residues critical for controlling channel activity are largely undefined, and *in vivo* mutant phenotypes have previously been described only for *Drosophila* (Kaplan and Trout, 1969; Warmke et al., 1991).

Imipramine and other structurally related tricyclic antidepressants reverse *egl-2(gf)* mutant phenotypes, but not those caused by *gf* mutations in other *C. elegans* potassium channel genes (Trent et al., 1983; Reiner et al., 1995; Weinshenker et al., 1995; our unpublished data), suggesting a specific interaction between tricyclics and EGL-2 channels. Tricyclic drugs are used to treat depression and other affective disorders, however their potential use is limited by many clinical side effects such as cardiac arrhythmia, weight fluctuation, constipation, and sexual dysfunction (Baldessarini, 1989; Kaplan et al., 1994). Tricyclics are thought to exert their therapeutic effect through chronic blockade of presynaptic serotonin and/or norepinephrine transporters (Frazer, 1997), but the molecular mechanisms mediating many of the deleterious side effects have not been identified. Previous studies have reported that some native K$^+$ currents can be blocked by tricyclics (Wooltorton and Mathie, 1993; Valenzuela et al., 1994; Kuo, 1998), but the molecular identities of these channels are unknown.

To investigate the mechanism of the *egl-2(gf)* phenotype and rescue by imipramine, we analyzed EGL-2 currents in *Xenopus* oocytes. Mutant EGL-2(*gf*) channels exhibited a negative shift in voltage dependence of activation, and both wild-type (WT) and mutant currents were blocked by imipramine. We hypothesize that EGL-2(*gf*) channels cause behavioral defects through suppression of excitability in critical cells. Consistent with this possibility, EGL-2::green fluorescent protein (GFP) fusions revealed *egl-2* expression in a subset of neurons and muscles that could explain the mutant behavioral defects. Suppression of *egl-2(gf)* phenotypes by imipramine likely results from the block of EGL-2(*gf*) channels. We suggest that a similar block of vertebrate EAG-like potassium channels may mediate some of the clinical side effects of tricyclic antidepressants.

MATERIALS AND METHODS

Behavioral assays. Chemotaxis assays were performed as described, with slight modifications (Bargmann et al., 1993). Eighteen- to 22-hr-old chemotaxis plates were allowed to dry coverless for 60 min before the assay, and 1 μl of 200 mM sodium azide was placed at the attractant and control spots to anesthetize the animals when they reached these spots. A minimum of three trials (at least 50 animals each) were performed for each genotype and attractant concentration. For the imipramine experiments, animals were grown on plates containing 0.7 ml of 2.4 mM imipramine (Sigma, St. Louis, MO) and assayed on chemotaxis plates (Bargmann et al., 1993) containing 315 μM imipramine. Statistical analysis was done using the unpaired Student's *t* test (Instat 2.01 for Macintosh).

Defecation assays were performed as described (Weinshenker et al., 1995). For each genotype, a minimum of 40 defecation cycles from at least three animals were assayed. Drug experiments were performed on plates containing 0.7 ml of 2.4 mM imipramine.

Anterior Mec assays were performed essentially as described (Chalfie and Sulston, 1981). Adult animals were picked individually to plates and assayed 45 min later. Each animal was tested for responsiveness to a light touch just posterior to the pharynx with an eyelash five times. For each genotype, at least 10 animals were touched five times each (one touch every 10 min). Imipramine experiments were performed on plates containing 0.7 ml of 2.4 mM imipramine.

Mutagenesis and mapping of egl-2(gf) *revertants.* Revertants of *egl-2(gf)* were isolated by mutagenizing *egl-2(n693sd)* and *egl-2(n2656sd)* with ethylmethanesulfonate (EMS) as described (Brenner, 1974) and screening for non-egg laying-defective (Egl) non-expulsion-defective (Exp) animals in the F2 generation. Transposon alleles of *egl-2(n693sd)* were similarly isolated by screening for revertants of *egl-2(n693sd)* in a *mut-6* mutator background. We isolated 30 EMS-induced alleles from 110,000 mutagenized genomes and three transposon insertion alleles from 90,000 mutagenized genomes. Four EMS-induced revertants of *egl-2(n693sd)*, *n904*, *n905*, *n906*, and *n907,* were kindly provided by C. Trent and H. R. Horvitz.

lon-2(e678) males were mated to revertant hermaphrodites, and F1 progeny were picked individually to plates and allowed to self-fertilize. F1 cross progeny were non-Egl non-Exp, indicating that the revertant alleles are *cis*-dominant. Broods containing *lon-2* mutants were screened for *egl-2(gf)* animals to assess linkage between *egl-2* and the suppressor. Approximately 1000 F2 progeny were screened for each revertant, and no *egl-2(gf)* animals were seen, indicating that all of the suppressors are tightly linked to *egl-2*.

egl-2 cloning. *egl-2(n693sd)* was mapped between *unc-34* and *unc-60* on the left arm of chromosome V (Trent et al., 1983; data not shown). Cosmids from the region (5 ng/μl) were coinjected with *rol-6(d)* marker DNA (200 ng/μl) into *egl-2(n905)* animals, and transgenic lines were established as described (Mello et al., 1991). *egl-2(n693sd)/egl-2(n905)* heterozygotes carrying the cosmid transgene were constructed, and partial suppression of the *egl-2(n693sd)* expulsion-defective (Exp) phenotype was obtained with cosmids ZK1005 and ZK1012. Overlapping regions from these cosmids were used to probe Southern blots of DNA from multiple *egl-2* alleles, and polymorphisms were identified in a 1.6 kb *Xba*I fragment in the *egl-2* alleles *sa373*, *sa400,* and *sa408*. This fragment was subcloned and sequenced, and the sequence was used to design primers for RT-PCR. Stratagene (La Jolla, CA) 5′ and 3′ rapid amplification of cDNA ends kits were used to obtain overlapping partial cDNAs, which were sequenced. *egl-2* genomic sequence was subsequently confirmed by the *C. elegans* Genome Sequencing Consortium (Coulson, 1996). Oligonucleotides for PCR and sequencing were from Life Technologies (Gaithersburg, MD). PCR was performed on a PTC-200 DNA engine from MJ Research. Sequencing was performed on an ABI PRISM dye terminator cycle sequencer by the Biochemistry Sequencing facility and the Pharmacology Sequencing facility at the University of Washington. For mutant *egl-2* alleles, PCR products from the *egl-2* gene using mutant and wild-type genomic DNA as template were gel-purified and sequenced. The *egl-2* cDNA GenBank accession number is AF130443.

Xenopus oocyte expression and electrophysiology. Three overlapping partial cDNAs were constructed by RT-PCR and cloned together into the pMXT oocyte expression vector (Wei et al., 1994). A silent mutation was introduced at base 2412 to create a *Spe*I site used in cloning. A full-length mouse *ether-a-go-go* (*meag*) clone (kindly provided by Barry Ganetzky) was cloned into the pMXT oocyte expression vector. The A478V mutation was introduced into the *egl-2* cDNA by overlap PCR mutagenesis (Horton et al., 1989). The cDNA was cloned into pMXT and sequenced

to confirm the change and rule out extraneous mutations. The A492V mutation in *meag* was similarly generated.

Capped cRNAs were generated by *in vitro* transcription using a commercial T3 RNA polymerase kit (mMessagemMachine; Ambion, Austin, TX) and linearized plasmid DNA templates. Oocyte isolation, injection, and handling followed standard procedures (Soreq and Seidman, 1992; Wei et al., 1994). Oocytes were injected with ∼50 ng (wild-type and mutant *egl-2*) or 10 ng (wild-type and mutant *meag*) cRNA. Wild-type and mutant EGL-2 currents were obtained in choline 96 (in mM: 96 choline Cl, 2 KCl, 1.8 CaCl$_2$, 1.0 MgCl$_2$, and 5 HEPES, pH 7.5) supplemented with 1.0 mM 4,4′-diisothiocyanato-stilbene-2,2′-disulfonic acid (Sigma) to block endogenous calcium-activated chloride currents (Barish, 1983) after 5–7 d of incubation at 19°C. Wild-type and mutant *meag* currents were obtained in ND96 (in mM: 96 NaCl, 2 KCl, 1.8 CaCl$_2$, 1.0 MgCl$_2$, and 5 HEPES, pH 7.5) after 1–3 d incubation at 19°C. Current recordings were digitally acquired by two-electrode voltage clamp with a Dagan TEV-200 amplifier and pClamp 7 (Axon Instruments, Foster City, CA). Current injection and voltage electrodes had resistances between 0.5 and 1.0 MΩ filled with 3 M KCl. Imipramine (Sigma) solutions were made in either choline 96 (wild-type and mutant EGL-2) or ND96 (wild-type and mutant MEAG) and exchanged with the bath solution by gravity flow. Data analysis was performed with Sigmaplot 4.0 (Jandel Scientific, Corte Madera, CA) and Origin 4.0 (Microcal).

GFP expression. For the short fusion, a PCR product containing 4.1 kb of upstream sequence, the first exon and intron, and part of the second intron of *egl-2* was inserted in frame into the pPD95.75 GFP expression vector (kindly provided by A. Fire, J. Ahnn, G. Seydoux, and S. Xu). For the full-length fusion, an *Nhe*I fragment from cosmid ZK1005 containing 5 kb upstream of *egl-2*, the entire *egl-2* coding region (10 kb), and 4.2 kb downstream of *egl-2* was cloned into the *Xba*I site of Bluescript (Stratagene). The GFP coding region was generated by PCR from pPD95.75 and cloned in frame into the *Age*I site in exon 13 of *egl-2* in the plasmid described above. The stop codon in GFP was mutated to a leucine codon so that the *egl-2* gene would be translated in its entirety. The short fusion (200 ng/μl) was coinjected with *lin-15(+)* DNA (60 ng/μl) into *lin-15(n765ts)* mutants, which have the multivulva (Muv) phenotype. Non-Muv transgenic lines were established, GFP was visualized, and cell identities were determined using epifluorescence microscopy and Nomarski optics. The long fusion (100 ng/μl) was linearized with *Sph*I and coinjected with *rol-6(d)* DNA (100 ng/μl) into wild-type animals. Rol transgenic lines were established, and serial images of L2 larvae were taken every 0.4 μm with a deconvoluting microscope using epifluorescence. Figure *5e* is a compressed image of the sum of 38 sections.

RESULTS

An *egl-2* gain-of-function mutation causes multiple behavioral phenotypes

Two independently isolated dominant gain-of-function (*gf*) mutations in the *C. elegans egl-2* gene (*n693* and *n2656*) inhibit egg-laying and enteric muscle contraction, leading to Egl and Exp phenotypes. These mutant phenotypes are rapidly rescued by exposure to tricyclic antidepressants such as imipramine, suggesting that the *egl-2* gene product is a tricyclic target. Pharmacological and cell ablation manipulations combined with behavioral assays suggest that the Egl and Exp defects are likely in the egg-laying and enteric muscles and not in the motor neurons that innervate them (Reiner et al., 1995; Weinshenker et al., 1995).

We tested *egl-2* mutants for chemotaxis to volatile odorants, a behavior that is mediated by amphid sensory neurons. *egl-2(gf)* mutants were defective in chemotaxis to both isoamyl alcohol and benzaldehyde, which are sensed by the AWC amphid neuron (Bargmann et al., 1993). Similar to the muscle defects, the isoamyl alcohol defect was rescued by imipramine (Fig. 1). Although *egl-2(gf)* has a weak locomotory defect, they were outperformed in this assay by the more severely locomotion-defective *unc-25* mutant (Fig. 1), suggesting that the *egl-2(gf)* chemotaxis defect is caused by sensory and not motor defects.
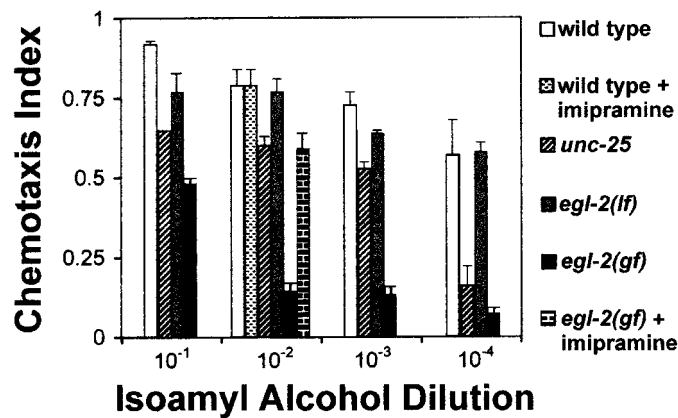
Figure 1. Volatile chemotaxis response of *egl-2* mutants to isoamyl alcohol. Chemotaxis indexes (CI) were calculated in the following way: CI = (number at attractant − number at control)/(total number) (Bargmann et al., 1993). Error bars indicate SD among individual trials. The *egl-2(gf)* allele was *egl-2(n693sd)*, the *egl-2(lf)* allele was *egl-2(n693sd sa236)*, and the *unc-25* allele was *unc-25(e156)*. Considering $p < 0.05$ as significant, *egl-2(lf)* is not significantly different from wild type at any dilution, *egl-2(gf)* is significantly different from wild type at every dilution, *unc-25(e156)* is significantly different from *egl-2(gf)* at all isoamyl alcohol dilutions except 10^{-4}, and *egl-2(gf)* + imipramine is significantly different from *egl-2(gf)*.

Table 1. Anterior Mec response of *egl-2* mutants

Genotype	Number of touches	% response
Wild-type	50	96
Wild-type + imipramine	50	100
egl-2(n693)	50	18
egl-2(n693) + imipramine	50	88
egl-2(sa236)	75	69

% response is the percentage of times that an animal responded by backing up when touched just posterior to the pharynx with an eyelash. Results for *egl-2(sa373)* were comparable to *egl-2(sa236)* (data not shown). *p* values were calculated using an ANOVA followed by a Newman–Keuls test and are as follows: wild-type vs wild-type + imipramine ($p > 0.05$), wild-type vs *egl-2(n693)* ($p < 0.001$), wild-type vs *egl-2(n693)* + imipramine ($p > 0.05$), wild-type + imipramine vs *egl-2(n693)* + imipramine ($p > 0.05$), *egl-2(n693)* vs *egl-2(n693)* + imipramine ($p < 0.001$), and wild-type vs *egl-2(sa236)* ($p < 0.01$).

egl-2(gf) mutants also had an imipramine-sensitive anterior mechanosensory-defective (Mec) phenotype, which is mediated by the ALM mechanosensory neurons (Chalfie and Sulston, 1981) (Table 1). Previously characterized male mating and locomotion defects in *egl-2(gf)* mutant are likely neuronally mediated, and these are also rescued by imipramine (Trent et al., 1983; Weinshenker et al., 1995; data not shown). These results demonstrate that an *egl-2(gf)* mutation can compromise neuronal and muscle function, and that its interaction with tricyclics is similar in the two tissues.

egl-2(gf) revertants define three classes of eag mutations

To determine the loss-of-function (*lf*) phenotype for *egl-2*, we mutagenized *egl-2(gf)* animals and isolated revertants that were no longer Egl or Exp. All revertants were tightly linked to *egl-2* (Materials and Methods), suggesting that they contain second site suppressors within the *egl-2* gene.

Table 2. Analysis of enteric muscle contraction in *egl-2* mutants

Genotype	% EMC
Wild-type	92
egl-2(n693sd)	0
egl-2(sa236)	97
egl-2(n693sd) + imipramine	86
egl-2(n693sd)/sDf34	7
egl-2(n693sd)/+	22
egl-2(n693sd)/Class I	0–8
egl-2(n693sd)/sa236	5
egl-2(n693sd)/Class II	20–24
egl-2(n693sd)/sa397	21
egl-2(n693sd)/Class III	37–57
egl-2(n693sd)/sa378	57

At least 40 defecation cycles were observed for each genotype. % enteric muscle contraction (% EMC) is the percentage of times a defecation motor program included a visible contraction of the enteric muscles. *egl-2(n693sd)* is a *gf* allele of *egl-2*. The deficiency *sDf34* used in this experiment deletes *egl-2* (data not shown) and genes on both sides of *egl-2*. Class I alleles: *n904, n905, n906, sa236, sa371, sa372, sa373, sa374, sa381, sa383, sa384, sa386, sa388, sa389, sa390, sa392, sa393, sa394, sa396,* and *sa407*. Class II alleles: *n907, sa382, sa397,* and *sa399*. Class III alleles: *sa375, sa377, sa378, sa380, sa385, sa387, sa391,* and *sa395*. Representative examples of each class (*sa236* for Class I, *sa397* for Class II, and *sa378* for Class III) in *trans* to *egl-2(n693sd)* are shown on the line below each class. The alleles *sa376, sa379,* and *sa400* fell between Class I and Class II, and *sa398* and *sa408* fell between Class II and Class III. *p* values, calculated using the Wilcoxon/Mann–Whitney *U* test (Instat 2.01 for Macintosh), are as follows: wild-type vs *egl-2(n693sd sa236)* ($p = 0.84$), wild-type vs *egl-2(n693sd)* + imipramine ($p = 0.31$), *egl-2(n693sd)/Df* vs *egl-2(n693sd)/+* ($p = 0.0002$).

To investigate the genetic properties of the revertants, we used the semidominance of the *egl-2(gf)* alleles in gene dosage tests. The enteric muscle contraction (EMC) defect of *egl-2(gf)* in *trans* to a deficiency of *egl-2* is more severe than the *gf* in *trans* to a wild-type copy of *egl-2* (Table 2). A null mutation of *egl-2* in *trans* to the *gf* would be expected to behave like a deficiency, whereas non-null mutations might give different results. We put each revertant in *trans* to *egl-2(gf)* and measured EMC defects (Table 2). The revertants fell into three classes. Class I alleles (20 alleles), such as *sa236*, behaved like an *egl-2* deficiency and probably are strong *lf* or null mutations. As homozygotes, *egl-2(sa236)* and other members of this class of revertants appear wild-type, having no gross defects in movement, feeding, fertility, defecation, egg laying, or chemotaxis to volatile odorants (Tables 1, 2, Fig. 1; data not shown). Class II alleles (four alleles) behaved like a wild-type copy of *egl-2*. Class III alleles (eight alleles) suppressed the *gf* to a greater degree than a wild-type allele, and thus are probably dominant-negative alleles.

egl-2 encodes a voltage-gated K$^+$ channel

To determine the role of *egl-2* in cell excitation and the nature of the tricyclic antidepressant interaction, we cloned *egl-2* (Materials and Methods). *egl-2* encodes an eag-like voltage-gated K$^+$ channel (VGK) (Fig. 2*a*) (GenBank accession number AF130443). The EGL-2 and *Drosophila* eag proteins are 54% identical in the N terminus, 75% identical in the transmembrane and pore domain, and 81% identical in the domain with homology to cyclic nucleotide-binding proteins (cNTP), but are divergent at the C terminus. The molecular lesion in the two independently isolated *egl-2(gf)* alleles is an A478V change in the S6 domain. This alanine is conserved among nearly all VGKs described to date, suggesting that this residue is critical for normal channel function (Fig. 2*b*). The Class I *sa236* mutation results in a stop codon at
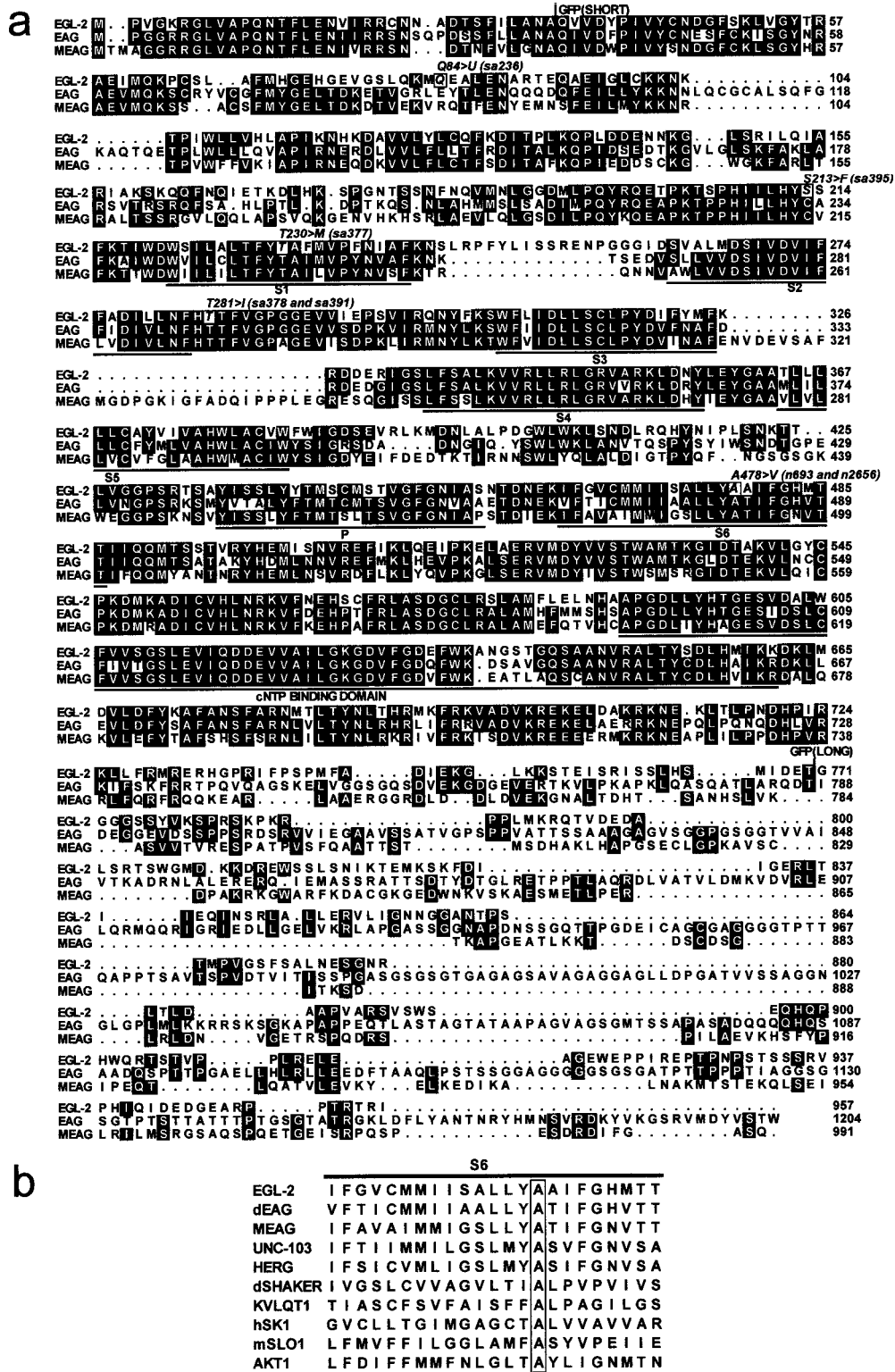
Figure 2. Alignment of EGL-2 with other K⁺ channels. *a,* Predicted amino acid sequence of the *egl-2* gene product and the molecular lesions found in mutant alleles aligned with *Drosophila* eag (EAG) and mouse eag (MEAG). The predicted transmembrane and pore domains are underlined, as is the region with homology to cyclic nucleotide-binding proteins (cNTP BINDING DOMAIN). Amino acid identities are *boxed* in *black*. Amino acids changed in mutant *egl-2* alleles are *outlined* in *black* and annotated on the line above. GFP fusion junctions are shown by *vertical gray lines*. *b,* Alignment of the sixth transmembrane domain (*S6*) of EGL-2 and other K⁺ channels. dEAG and dSHAKER are *Drosophila* channels, UNC-103 is a *C. elegans erg* homolog, HERG (human *erg*; mutated in long QT syndrome), KVLQT1 (mutated in long QT syndrome), and hSK1 (small conductance Ca^{2+}-activated K⁺ channel) are human channels, mSLO is a mouse large conductance Ca^{2+}-activated K⁺ channel, and AKT1 is an *Arabidopsis* inward-rectifying K⁺ channel. The alanine that is mutated in *egl-2(gf)* alleles and the corresponding residues in other channels are *boxed*. GenBank accession numbers for sequences used: EGL-2 (AF130443), MEAG (UO4294), *Drosophila* EAG (M61157), *Drosophila* Shaker (M17211), UNC-103 (Z35596), HERG (UO4270), KVLQT1 (U89364), hSK1 (AF131938), mSLO (L16912), and AKT1 (X62907).
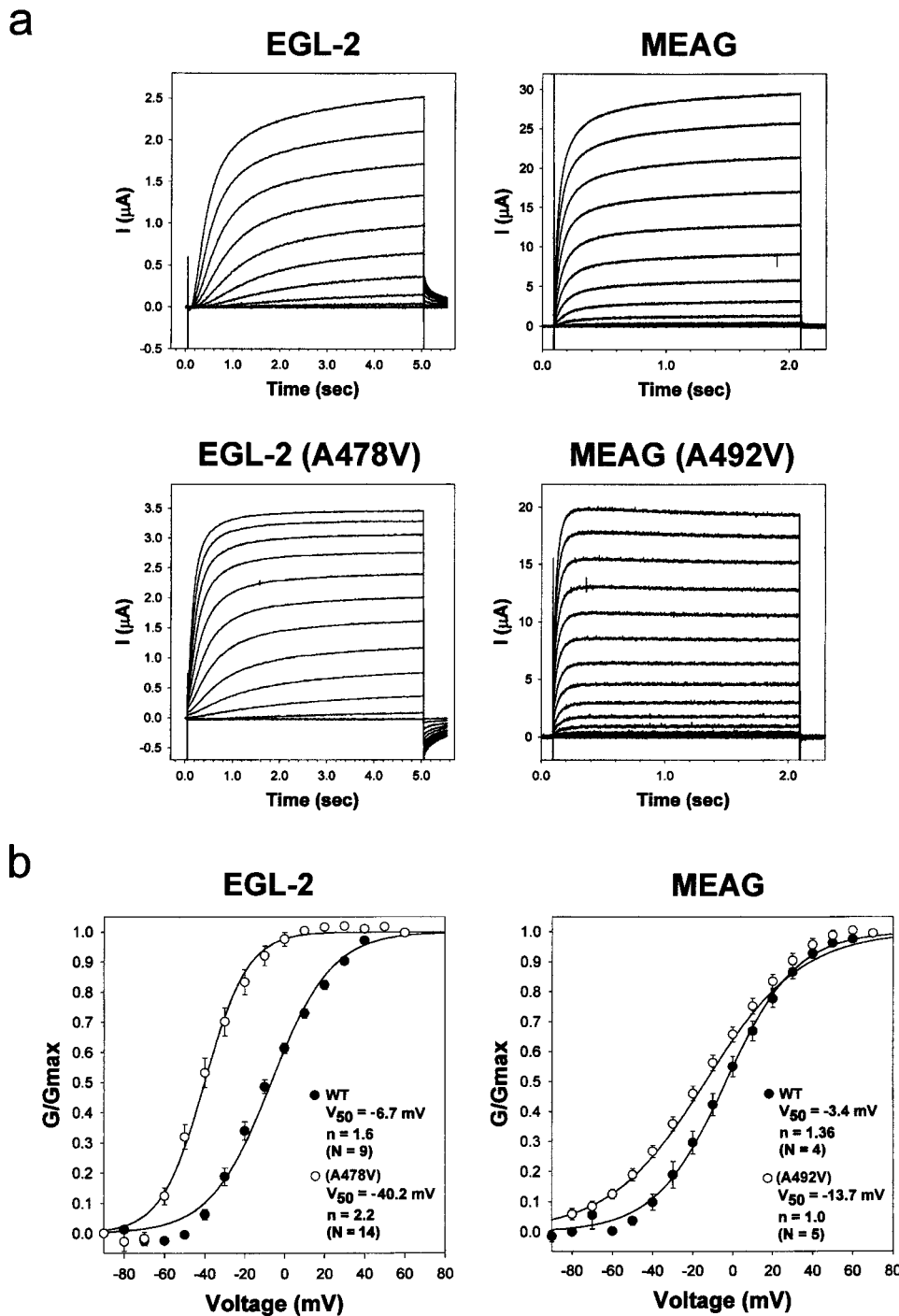
a

Figure 3. Functional properties of wild-type and gain-of-function EGL-2 and MEAG K⁺ channels in *Xenopus* oocytes assayed by two-electrode voltage-clamp. *a,* Current records from oocytes injected with wild-type *egl-2*, gain-of-function *egl-2(A478V)*, and corresponding *meag* and *meag(A492V)* cRNAs. Currents evoked by families of voltage steps from a holding potential of −100 mV, in 10 mV increments [−90 to +40 mV for *egl-2* and *egl-2(A478V)*); −90 to +50 mV for MEAG and MEAG(A492V)]. Outward tail currents observed from wild-type EGL-2 channels resulted from a repolarization step to −50 mV. A −100 mV repolarization step was used for all other channels. *b,* Normalized conductance–voltage relationships. Conductances were calculated from current amplitudes at the end of 5 sec [EGL-2 and EGL-2(A478V)] and 2 sec [MEAG and MEAG(A492V)] voltage steps, based on a reversal potential of −90 mV in ND96. Individual data sets were fitted by a single Boltzmann function, $G/G_{max} = (1 + \exp(-n(V - V_{50})/kT))^{-1}$, where *n* is the slope factor reflecting intrinsic voltage sensitivity, V_{50} is the voltage at half-maximal conductance, and *T* is absolute temperature. Mean values were plotted with SEM.

amino acid 84 (Fig. 2*a*), and thus is probably a null allele. We identified molecular lesions for four Class III dominant negative alleles. These lesions all cause single missense mutations affecting residues near S1 and S2: S213F (*sa395*), T230M (*sa377*), and T285I (*sa378* and *sa391*) (Fig. 2*a*).

S6 mutation shifts voltage dependence of activation for EGL-2 and murine MEAG channels

To investigate the mechanism underlying the *in vivo* phenotype of the *egl-2(gf)* mutations, we studied the properties of WT and *gf* mutant (A478V) EGL-2 channels expressed in *Xenopus* oocytes. Oocytes injected with wild-type *egl-2* cRNA expressed voltage-

dependent, noninactivating potassium currents characterized by unusually slow activation kinetics, requiring voltage steps of 5 sec to approach steady-state (Fig. 3*a*). A conductance–voltage (*G–V*) plot of WT EGL-2 currents revealed a voltage of half-maximal activation (V_{50}) of −7 mV, centered within a voltage-operating range of ~80 mV (Fig. 3*b*). Oocytes injected with mutant *egl-2(A478V)* cRNA expressed similar nonactivating potassium currents, but with altered voltage dependence of activation (Fig. 3*a*). *G–V* plots for A478V EGL-2 channels revealed a V_{50} of −40 mV, a shift of −33 mV relative to WT EGL-2 channels (Fig. 3*b*). This hyperpolarized shift in the V_{50} of A478V EGL-2 channels allows a significant fraction of available mutant channels to be activated
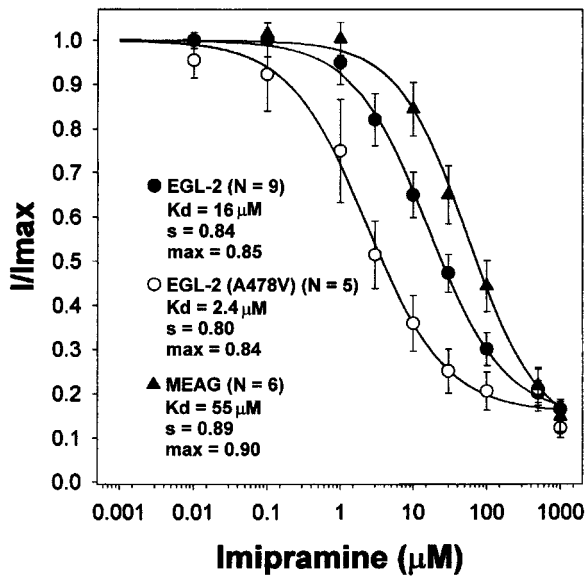
Figure 4. Imipramine inhibits EGL-2 and MEAG channels. Dose–response plots for wild-type EGL-2, EGL-2(A478V), and MEAG currents, measured at 40 mV, at the end of 5 sec [EGL-2 and EGL-2(A478V)] and 2 sec (MEAG) voltage steps from a holding potential of −100 mV. Individual data sets normalized to maximal current evoked in ND96 and fitted by the Hill function, $I = 1 - (max/(1 + (K_d/[\text{imipramine}])^s))$, where *max* is the maximal fractional inhibition, K_d is the imipramine concentration at half-maximal inhibition, and *s* is the slope factor. Mean values were plotted with SEM.

at hyperpolarized potentials. This is consistent with the observed mutant behavioral phenotypes of *egl-2*(*gf*) mutants, because a muscle or neuron expressing these mutant channels may be hyperpolarized and unable to respond appropriately to excitatory stimuli.

A478 is positioned near residues thought to undergo gating-dependent conformational changes in the Shaker potassium channel (Liu et al., 1997; Holmgren et al., 1998). We therefore tested the ability of the A478V substitution to confer a *gf* phenotype in the murine *eag* homolog *meag* (Warmke and Ganetzky, 1994), by engineering an analogous missense mutation in MEAG (A492V). A492V MEAG channels exhibited a *G–V* shifted toward hyperpolarized potentials ($V_{50} = -13.7$ mV) relative to WT MEAG ($V_{50} = -3.4$ mV) (Fig. 3*a,b*), demonstrating a modest, but functionally similar effect of this substitution in a mouse *eag*-like channel

Imipramine blocks EGL-2 and MEAG channels

To determine the mechanism of imipramine rescue of the *egl-2*(*gf*) phenotypes, we assessed its ability to block EGL-2 channels in oocytes. Imipramine was able to block both WT and A478V EGL-2 channels (Fig. 4). The derived Hill coefficients (s = 0.84, WT; s = 0.80, A478V) suggest a binding stoichiometry of one imipramine molecule to one channel. Similar results were obtained with WT MEAG channels (Fig. 4), except that imipramine inhibits WT MEAG currents with an ~10-fold lower potency ($K_d = 55$ μM) than EGL-2 currents.

Block by imipramine at each test concentration was rapid and essentially complete within the ~2 min allowed for equilibration between exchanges of bath solutions, at the holding potential of −100 mV. A variable secondary component of block was observed with much slower kinetics, perhaps reflecting state depen-
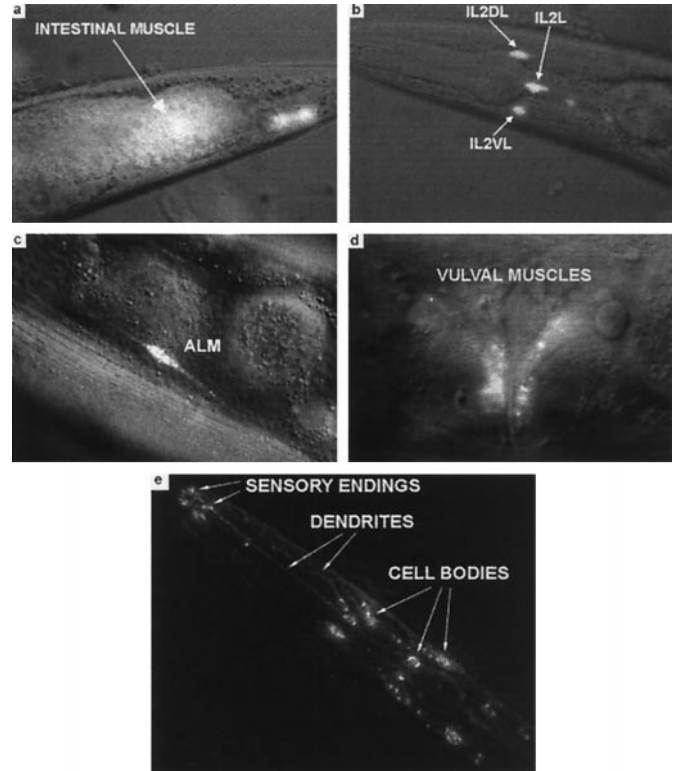

Figure 5. *egl-2* expression. Anterior is left, dorsal is up. Merged Nomarski and GFP fluorescence images. *a,* Short EGL-2::GFP expression in the intestinal muscles (posterior end of an adult animal). GFP-expressing cells posterior to the intestinal muscle are the tail neurons ALN and PLN in a slightly lower focal plane. *b,* Short EGL-2::GFP expression in neurons in the lateral ganglion (anterior end of the animal). Posterior to the IL2 neurons, BAGL and AWCL are also visible, but faint. Other GFP-expressing cells in this region are either faint or out of focus. *c,* Long EGL-2::GFP expression in the ALM mechanosensory neurons. *d,* Long EGL-2::GFP expression in the vulval muscles used for egg laying. *e,* Deconvoluted image of full-length EGL-2::GFP fusion expression in sensory neuron endings.

dence of block (Kuo, 1998). This secondary component of block may account for the residual 10% of channels not blocked with our assay conditions (Fig. 4). Block was not observed to be reversible by washes of up to 30 min, consistent with a slow off-rate of imipramine. The rapid and dose-dependent inhibition of EGL-2 and MEAG channels provides evidence that imipramine directly blocks these channels and suggests that imipramine may block other EAG-like channels with similar efficacy.

EGL-2::GFP fusions are expressed in muscle and neurons

To determine the cellular expression pattern of *egl-2*, we constructed two EGL-2::GFP fusions (Materials and Methods; Fig. 2*a*). Consistent with the Exp defect of *egl-2*(*gf*) mutants, the short fusion (4.1 kb of upstream *egl-2* sequence) was expressed in the intestinal muscles, which are two of the four enteric muscles (Fig. 5*a*). We hypothesize that inappropriately activated EGL-2 K$^+$ channels in these muscles compromise their ability to depolarize and contract. In addition to the muscle expression, the short fusion was expressed in the AFD, ALN, AQR, ASE, AWC, BAG, IL2, PLN, PQR, and URX neurons in hermaphrodites and males, and in a subset of ray sensory neurons in males (Fig. 5*b;* data not shown). The expression in AWC is consistent with the
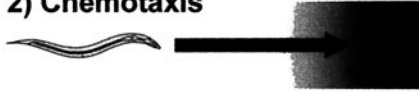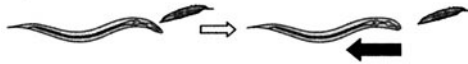
egl-2(gf) BEHAVIORAL DEFECTS

BEHAVIOR | **EGL-2::GFP LABELED CELLS** | **IMIPRAMINE RESCUE**

1) Egg-laying → **Vulval Muscles** — Yes

2) Chemotaxis → **Chemosensory Neuron (AWC)** — Yes

3) Anterior Touch Response → **Mechanosensory Neuron (ALM)** — Yes

4) Defecation Motor Program — Exp — **Enteric Muscles** — Yes
Enteric Muscle Contraction (EMC)

Figure 6. Summary of *egl-2(gf)* phenotypes, EGL-2 expression, and rescue by imipramine. Mutant EGL-2 channels are expressed in muscle and neurons and cause excitation defects by allowing an inappropriate efflux of K$^+$ in these cells. Imipramine rescues *egl-2(gf)* phenotypes by blocking the mutant channels and restoring excitability.

chemotaxis defect in *egl-2*(*gf*) mutants (Fig. 1). Because ray neurons are involved in mating (Liu and Sternberg, 1995), *egl-2* expression in rays may underlie the previously characterized male mating defect of *egl-2(gf)* mutants (Trent et al., 1983).

The long fusion (5 kb of upstream *egl-2* sequence, the entire 10 kb *egl-2* coding region, and 4.2 kb of downstream *egl-2* sequence) was highly localized at dendritic endings of neurons in the nose, but only faintly in the processes (Fig. 5*e*). This localization is probably in the ciliated endings of head sensory neurons. Neuronal cell bodies in the lateral ganglion also label with this fusion (Fig. 5*e*). This fusion was also expressed in the ALM mechanosensory neurons (Fig. 5*c*), which can explain the *egl-2*(*gf*) anterior Mec phenotype (Table 1). Consistent with the Egl defect of *egl-2*(*gf*) mutants, we saw occasional expression of this fusion in the vulval muscles used for egg laying (Fig. 5*d*).

DISCUSSION

egl-2 encodes a voltage-gated K$^+$ channel that is blocked by the tricyclic antidepressant imipramine. The *egl-2*(*gf*) mutation produces a negative shift in the voltage dependence of activation of EGL-2 channels, thus increasing the likelihood of open channels at hyperpolarized potentials. We propose that the *egl-2*(*gf*) phenotypes result from an inappropriate suppression of excitability in cells that express the mutant channel. Imipramine blocks the mutant channel and restores function by inhibiting the suppression of excitability. This model is supported by the close parallel between behavioral defects in *egl-2*(*gf*) mutants and EGL-2::GFP expression in cells that mediate these behaviors (Fig. 6).

egl-2(lf) phenotypes

We did not detect any gross behavioral defects in *egl-2*(*lf*) mutants. We speculate that there are many K$^+$ channels with overlapping functions in the excitable cells of *C. elegans*, and that loss of any one of them does not greatly affect cellular excitability. Conversely, activation of some of these channels causes an excit-

ability phenotype out of proportion to their wild-type contribution. This generalization is supported by the severe phenotypes caused by *gf* mutations, in contrast to mild or absent phenotypes caused by *lf* mutations, in other *C. elegans* K$^+$ channels (Reiner et al., 1995; Elkes et al., 1997; Johnstone et al., 1997).

EGL-2 expression

The expression of the short EGL-2::GFP fusion in two of the four enteric muscles is consistent with the enteric muscle contraction defect of *egl-2*(*gf*) mutants. Vulval muscle labeling was observed in occasional animals expressing the long fusion, which can explain the Egl defect in *egl-2*(*gf*) mutants. This is consistent with the pharmacology of the *egl-2*(*gf*) Egl phenotype, as agonists that act directly on the egg-laying muscles to promote egg laying in the wild type fail to do so in *egl-2*(*gf*) mutants (Trent et al., 1983; Weinshenker et al., 1995). Interestingly, nearly all neurons that express the fusions are sensory neurons, suggesting that *egl-2* serves a common function in *C. elegans* sensory neurons of different modalities.

Like the long EGL-2::GFP fusion, components of the odorant-sensing machinery are localized to the ciliated endings of amphid sensory neurons (Coburn and Bargmann, 1996; Sengupta et al., 1996; Colbert et al., 1997; Roayaie et al., 1998). It is possible that EGL-2 functions in sensory endings and is modulated by components of sensory transduction. *Drosophila eag* mutants are defective in odorant response (Dubin et al., 1998), and rat *eag* is expressed in the olfactory bulb (Ludwig et al., 1994), suggesting conservation of an eag function in olfaction. In addition, bovine *eag* is expressed in retinal photoreceptors and may encode the native I_{Kx} current, suggesting a general role for eag in sensory transduction processes (Frings et al., 1998).

K$^+$ channel structure and function

Voltage-gated K$^+$ channels display a remarkable heterogeneity of intrinsic properties, reflected in the molecular diversity of K$^+$ channel genes (Wei et al., 1996). The fact that the EGL-2 S6 alanine 478 is highly conserved among all families of VGKs

suggests that it is critical for some aspect of normal channel function. This is supported by the *gf* shifts in *G–V* conferred by a modest change to a valine in EGL-2 and MEAG. Changing the analogous alanine in KVLQT1 channels to valine or glutamate results in the cardiac arrhythmia long QT syndrome, a probable dominant-negative phenotype (Wang et al., 1996; Shalaby et al., 1997). These mutations focus attention on S6 as an important structure mediating channel function.

Examples of S6 amino acid substitution that either stabilize channel open states or accelerate transitions from closed to open states have been observed in a wide variety of other K$^+$ channels. These include *Shaw* K$^+$ channels (Elkes et al., 1997; Johnstone et al., 1997), *Slo*-type calcium-activated K$^+$ channels (Lagrutta et al., 1994), the yeast YKC1 K$^+$ channel (Loukin et al., 1997), and the *Shaker* K$^+$ channel (Liu et al., 1997; Holmgren et al., 1998). Our data suggest that elements of the gating mechanism mediated by S6 may be conserved between K$^+$ channels from diverse gene families. This suggestion is supported by the conserved "inverted teepee" structural motif revealed by the crystal structures of the Kcsa K$^+$ channel from *Streptomyces lividans* (Doyle et al., 1998) and the MscL cation channel from *Mycobacterium tuberculosis* (Chang et al., 1998). In both structures, the ion conduction pathway is lined by a single tilted transmembrane α-helix contributed by each subunit. This critical α-helix is TM2 for Kcsa, TM1 for MscL and, by analogy, S6 for voltage-gated K$^+$ channel subunits. Rotation and translational movements of TM1 and TM2 underlie pH-dependent gating of the Kcsa channel (Perozo et al., 1999) and may provide a conserved structural mechanism used for gating in other potassium channels. Mutations of critical S6 residues could affect gating properties by influence the energetics of these conformational changes. Our data with *egl-2* and *meag* are consistent this possibility.

The *egl-2*(*gf*) revertants may provide information about K$^+$ channel structure and function. The Class II revertants restore relatively normal function to the *gf* mutant channels. These are probably second site mutations that compensate for the *gf* mutation, and they potentially provide mechanistic information about channel gating. The Class III alleles behave as dominant negatives. These mutations may suppress the *gf* mutation by directly or allosterically countering the action of A478V in S6. Alternatively, the suppressors could inhibit proper channel folding or processing independent of A478V. These alleles may provide a useful *in vivo* model for studying dominant-negative K$^+$ channel subunit interactions.

Imipramine block of *eag* channels

We show that EGL-2 and MEAG channels are rapidly blocked by externally applied imipramine in a saturable fashion, with a high affinity in the range of 10–100 μM. These properties are in agreement with previous studies describing imipramine block of native K$^+$ channels from cardiac myocytes (Isenberg and Tamargo, 1985), peripheral sensory neurons (Ogata and Tatebayashi, 1993; Wooltorton and Mathie, 1993, 1995), and hippocampal neurons (Kuo, 1998). Both noninactivating and transient native potassium currents are blocked by imipramine, depending on the tissue source. All reported native imipramine-sensitive currents tested have binding constants in the range of 10–100 μM and a putative external binding site. Our results suggest that these imipramine-sensitive currents may be encoded by K$^+$ channel genes of the EAG gene family. Consistent with this possibility, heterologous expression studies reveal that the EAG gene family is capable of producing homomeric K$^+$ channels with a diversity

of kinetic properties, encompassing both noninactivating (eag, erg, elk subfamilies) and transient (erg, elk subfamilies) channel types (Shi et al., 1997, 1998; Engeland et al., 1998). Among *gf* mutations in *C. elegans* that have been shown or hypothesized to activate K$^+$ channels, *egl-2*(*gf*) is the only one that is rescued by imipramine (Reiner et al., 1995; Elkes et al., 1997; Johnstone et al., 1997), suggesting a specific tricyclic-EAG interaction. The higher concentrations of imipramine required to rescue *egl-2*(*gf*) behavioral defects *in vivo* (~25 μM; E. Round, personal communication) than to block EGL-2 *in vitro* (~10 μM) is likely due to the general impermeability of the *C. elegans* cuticle (Lewis et al., 1980). Should imipramine show specificity for K$^+$ channels encoded by the EAG gene family, it may provide an attractive molecular substrate for the rational design of blocking agents that target members of this family (Mathie et al., 1998).

EAG channels, tricyclic antidepressants, and human disease

The interaction between tricyclic antidepressants and EGL-2 provides a link that may explain one of the most common side effects of these psychotropic drugs. Long QT syndrome is a cardiac arrhythmia that can either be inherited or caused by drugs that block K$^+$ channels (Tan et al., 1995). One inherited form is associated with dominant-negative mutations in *HERG*, a VGK in the EAG gene family that encodes the cardiac I_{Kr} K$^+$ current (Sanguinetti et al., 1995; Trudeau et al., 1995). Tricyclics can cause long QT syndrome, and we speculate that they may do so in part by blocking HERG channels. In support of this model, imipramine can significantly block I_{Kr} currents in ventricular myocytes at concentrations found in the serum of patients taking clinical doses of the drug (~1 μM; Baldessarini, 1989; Valenzuela et al., 1994). In addition, a human eag channel (h-*eag*) has recently been cloned, and both h-*eag* and rat *eag* channels are expressed in brain (Ludwig et al., 1994; Occhiodoro et al., 1998). h-*eag* and *meag* are 100% conserved in the transmembrane and pore regions, indicating that imipramine probably blocks h-*eag* channels. Our results suggest that acute cardiac and neurological side effects of imipramine use may result from the block of HERG, h-eag, or other K$^+$ channels encoded by the EAG gene family.

Putative targets of psychotropic drugs have been determined traditionally by assaying binding to known receptors *in vitro*. The combination of genetics and pharmacology in *C. elegans* offers an alternative means to identify and study these targets *in vivo*.

REFERENCES

Adelman JP, Bond CT, Pessia M, Maylie J (1995) Episodic ataxia results from voltage-dependent potassium channels with altered functions. Neuron 15:1449–1454.

Baldessarini RJ (1989) Current status of antidepressants: clinical pharmacology and therapy. J Clin Psychiatry 50:117–126.

Bargmann CI, Hartwieg E, Horvitz HR (1993) Odorant-selective genes and neurons mediate olfaction in *C. elegans*. Cell 74:515–527.

Barish ME (1983) A transient calcium-dependent chloride current in the immature *Xenopus* oocyte. J Physiol (Lond) 342:309–325.

Brenner S (1974) The genetics of *Caenorhabditis elegans*. Genetics 77:71–94.

Bruggemann A, Pardo LA, Stuhmer W, Pongs O (1993) Ether-a-go-go encodes a voltage-gated channel permeable to K$^+$ and Ca^{2+} and modulated by cAMP. Nature 365:445–448.

Chalfie M, Sulston J (1981) Developmental genetics of the mechanosensory neurons of *Caenorhabditis elegans*. Dev Biol 82:358–370.

Chang G, Spencer RH, Lee AT, Barclay MT, Rees DC (1998) Structure of the MscL homolog from Mycobacterium tuberculosis: A gated mechanosensitive ion channel. Science 282:2220–2226.

Coburn CM, Bargmann CI (1996) A putative cyclic nucleotide-gated channel is required for sensory development and function in *C. elegans*. Neuron 17:695–706.

Colbert HA, Smith TL, Bargmann CI (1997) OSM-9, a novel protein with structural similarity to channels, is required for olfaction, mechanosensation, and olfactory adaptation in *Caenorhabditis elegans*. J Neurosci 17:8259–8269.

Coulson A (1996) The *Caenorhabditis elegans* genome project. *C. elegans* genome consortium. Biochem Soc Trans 24:289–291.

Curran ME, Splawski I, Timothy KW, Vincent GM, Green ED, Keating MT (1995) A molecular basis for cardiac arrhythmia: HERG mutations cause long QT syndrome. Cell 80:795–803.

Doyle DA, Morais Cabral J, Pfuetzner RA, Kuo A, Gulbis JM, Cohen SL, Chait BT, MacKinnon R (1998) The structure of the potassium channel: molecular basis of K$^+$ conduction and selectivity. Science 280:69–77.

Dubin AE, Liles MM, Harris GL (1998) The K$^+$ channel gene *ether a go-go* is required for the transduction of a subset of odorants in adult *Drosophila melanogaster*. J Neurosci 18:5603–5613.

Elkes DA, Cardozo DL, Madison J, Kaplan JM (1997) EGL-36 Shaw channels regulate *C. elegans* egg-laying muscle activity. Neuron 19:165–174.

Engeland B, Neu A, Ludwig J, Roeper J, Pongs O (1998) Cloning and functional expression of rat ether-a-go-go-like K+ channel genes. J Physiol (Lond) 513:647–654.

Frazer A (1997) Pharmacology of antidepressants. J Clin Psychopharmacol 17:2S–18S.

Frings SJ, Brull N, Dzeja C, Angele A, Hagen V, Kaupp UB, Baumann A (1998) Characterization of ether-a-go-go channels present in photoreceptors reveals similarity to IKx, a K+ current in rod inner segments. J Gen Physiol 111:583–599.

Ganetzky B, Robertson GA, Wilson GF, Trudeau MC, Titus SA (1999) The eag family of K$^+$ channels in *Drosophila* and mammals. Ann NY Acad Sci 868:356–369.

Holmgren M, Shin KS, Yellen G (1998) The activation gate of a voltage-gated K$^+$ channel can be trapped in the open state by an intersubunit metal bridge. Neuron 21:617–621.

Horton RM, Hunt HD, Ho SN, Pullen JK, Pease LR (1989) Engineering hybrid genes without the use of restriction enzymes: gene splicing by overlap extension. Gene 77:61–68.

Isenberg G, Tamargo J (1985) Effect of imipramine on calcium and potassium currents in isolated bovine ventricular myocytes. Eur J Pharmacol 108:121–131.

Johnstone DB, Wei A, Butler A, Salkoff L, Thomas JH (1997) Behavioral defects in *C. elegans egl-36* mutants result from potassium channels shifted in voltage-dependence of activation. Neuron 19:151–164.

Kaplan WD, Trout WE III (1969) The behavior of four neurological mutants of *Drosophila*. Genetics 61:399–409.

Kaplan HI, Sadock BJ, Grebb JA (1994) Major depressive disorder and bipolar I disorder. In: Synopsis of psychiatry (Retford DC, ed), pp 516–555. Baltimore: Williams and Wilkins.

Kuo CC (1998) Imipramine inhibition of transient K$^+$ current: an external open channel blocker preventing fast inactivation. Biophys J 12:2845–2857.

Lagrutta A, Shen KZ, North RA, Adelman JP (1994) Functional differences among alternatively spliced variants of *Slowpoke*, a *Drosophila* calcium-activated potassium channel. J Biol Chem 269:20347–20351.

Lewis JA, Wu C-H, Berg H, Levine JH (1980) The genetics of levamisole resistance in the nematode *Caenorhabditis elegans*. Genetics 95:905–928.

Liu KS, Sternberg PW (1995) Sensory regulation of male mating behavior in *Caenorhabditis elegans*. Neuron 14:79–89.

Liu Y, Holmgren M, Jurman ME, Yellen G (1997) Gated access to the pore of a voltage-dependent K$^+$ channel. Neuron 19:175–84.

Loukin SH, Vaillant B, Zhou XL, Spalding EP, Kung C, Saimi Y (1997) Random mutagenesis reveals a region important for gating of the yeast K$^+$ channel Ykc1. EMBO J 16:4817–4825.

Ludwig J, Terlau H, Wunder F, Bruggemann A, Pardo LA, Marquardt A, Stuhmer W, Pongs O (1994) Functional expression of a rat homolog of the voltage gated *ether a go-go* potassium channel reveals differences in selectivity and activation kinetics between the *Drosophila* channel and its mammalian counterpart. EMBO J 13:4451–4458.

Mathie A, Wooltorton JR, Watkins CS (1998) Voltage-activated potassium channels in mammalian neurons and their block by novel pharmacological agents. Gen Pharmacol 30:13–24.

Mello CC, Kramer JM, Stinchcomb D, Ambros V (1991) Efficient gene transfer in *C. elegans*: extrachromosomal maintenance and integration of transforming sequences. EMBO J 10:3959–3970.

Occhidoro T, Bernheim L, Liu J-H, Bijlenga P, Sinnreich M, Bader CR, Fischer-Lougheed J (1998) Cloning of a human *ether-a-go-go* potassium channel expressed in myoblasts at the onset of fusion. FEBS Lett 434:177–182.

Ogata N, Tatebayashi H (1993) Differential inhibition of a transient K$^+$ current by chlorpromazine and 4-aminopyridine in neurons of the rat dorsal root ganglia. Br J Pharmacol 109:1239–1246.

Perozo E, Cortes DM, Cuello LG (1999) Structural rearrangements underlying K$^+$-channel activation gating. Science 285:73–78.

Reiner DJ, Weinshenker D, Thomas JH (1995) Analysis of dominant mutations affecting muscle excitation in *Caenorhabditis elegans*. Genetics 141:961–976.

Roayaie K, Crump JG, Sagasti A, Bargmann CI (1998) The G alpha protein ODR-3 mediates olfactory and nociceptive function and controls cilium morphogenesis in *C. elegans* olfactory neurons. Neuron 20:55–67.

Sanguinetti MC, Jurkiewicz NK (1990) Two components of cardiac delayed rectifier K$^+$ current. Differential sensitivity to block by class III antiarrhythmic agents. J Gen Physiol 96:195–215.

Sanguinetti MC, Jiang C, Curran ME, Keating MT (1995) A mechanistic link between an inherited and an acquired cardiac arrhythmia: *HERG* encodes the I_{Kr} potassium channel. Cell 81:299–307.

Schonherr R, Hehl S, Terlau H, Baumann A, Heinemann SH (1999) Individual subunits contribute independently to slow gating of bovine EAG potassium channels. J Biol Chem 274:5362–5369.

Sengupta P, Chou JH, Bargmann CI (1996) odr-10 encodes a seven transmembrane domain olfactory receptor required for responses to the odorant diacetyl. Cell 84:899–909.

Shalaby FY, Levesque PC, Yang WP, Little WA, Conder ML, Jenkins-West T, Blanar MA (1997) Dominant-negative *KvLQT1* mutations underlie the LQT1 form of long QT syndrome. Circulation 96:1733–1736.

Shi W, Wymore RS, Wang HS, Pan Z, Cohen IS, McKinnon D, Dixon JE (1997) Identification of two nervous system-specific members of the erg potassium channel gene family. J Neurosci 17:9423–9432.

Shi W, Wang HS, Pan Z, Wymore RS, Cohen IS, McKinnon D, Dixon JE (1998) Cloning of a mammalian elk potassium channel gene and EAG mRNA distribution in rat sympathetic ganglia. J Physiol (Lond) 511:675–682.

Soreq H, Seidman S (1992) Xenopus oocyte microinjection: from gene to protein. Methods Enzymol 207:225–265.

Stansfeld CE, Roper J, Ludwig J, Weseloh RM, Marsh SJ, Brown DA, Pongs O (1996) Elevation of intracellular calcium by muscarinic receptor activation induces a block of voltage-activated rat *ether-a-go-go* channels in a stably transfected cell line. Proc Natl Acad Sci USA 93:9910–9914.

Tan HL, Hou CJ, Lauer MR, Sung RJ (1995) Electrophysiologic mechanisms of the long QT interval syndromes and torsade de pointes. Ann Intern Med 122:701–714.

Terlau H, Ludwig J, Steffan R, Pongs O, Stuhmer W, Heinemann SH (1996) Extracellular Mg^{2+} regulates activation of rat *eag* potassium channel. Pflügers Arch 432:301–312.

Trent C, Tsung N, Horvitz HR (1983) Egg-laying defective mutants of the nematode *C. elegans*. Genetics 104:619–647.

Trudeau MC, Warmke JW, Ganetzky B, Robertson GA (1995) HERG, a human inward rectifier in the voltage-gated potassium channel family. Science 269:92–95.

Valenzuela C, Sanchez-Chapula J, Delpon E, Elizalde A, Perez O, Tamargo J (1994) Imipramine blocks rapidly activating and delays slowly activating K$^+$ current activation in guinea pig ventricular myocytes. Circ Res 74:687–699.

Vetter DE, Mann JR, Wangemann P, Liu J, McLaughlin KJ, Lesage F, Marcus DC, Lazdunski M, Heinemann SF, Barhanin J (1996) Inner ear defects induced by null mutation of the isk gene. Neuron 17:1251–1264.

Wang Q, Curran ME, Splawski I, Burn TC, Millholland JM, VanRaay TJ, Shen J, Timothy KW, Vincent GM, de Jager T, Schwartz PJ, Toubin

JA, Moss AJ, Atkinson DL, Landes GM, Connors TD, Keating MT (1996) Positional cloning of a novel potassium channel gene: *KVLQT1* mutations cause cardiac arrhythmias. Nat Genet 12:17–23.

Warmke J, Drysdale R, Ganetzky B (1991) A distinct potassium channel polypeptide encoded by the *Drosophila* eag locus. Science 252:1560–1562.

Warmke JW, Ganetzky BA (1994) Family of potassium channel genes related to eag in *Drosophila* and mammals. Proc Natl Acad Sci USA 91:3438–3442.

Wei A, Solaro C, Lingle C, Salkoff L (1994) Calcium sensitivity of BK-type K$_{Ca}$ channels determined by a separable domain. Neuron 13:671–681.

Wei A, Jegla T, Salkoff L (1996) Eight potassium channel families revealed by the *C. elegans* genome project. Neuropharmacology 35:805–829.

Weinshenker D, Garriga G, Thomas JH (1995) Genetic and phamacological analysis of neurotransmitters controlling egg laying in *C. elegans*. J Neurosci 15:6975–6985.

Wooltorton JRA, Mathie A (1993) Block of potassium currents in rat isolated sympathetic neurones by tricyclic antidepressants and structurally related compounds. Br J Pharmacol 110:1126–1132.

Wooltorton JR, Mathie A (1995) Potent block of potassium currents in rat isolated sympathetic neurones by the uncharged form of amitriptyline and related tricyclic compounds. Br J Pharmacol 116:2191–2200.